Mass Transfer and Radical Flux Effects in Dispersed-Phase Polymerization of Isooctyl Acrylate

Alan J. Back, F. Joseph Schork

School of Chemical and Biomolecular Engineering, Georgia Institute of Technology, Atlanta, Georgia 30332-0100

Received 20 March 2006; accepted 2 July 2006
DOI 10.1002/app.25029
Published online in Wiley InterScience (www.interscience.wiley.com).

ABSTRACT: The kinetics of dispersed phase polymerization of a highly water-insoluble monomer (isooctyl acrylate) were explored in emulsion, miniemulsion, and microsuspension polymerization. The effects of monomer water solubility and choice of initiator (oil- vs. water-soluble) strongly impact the final product (particle size and molecular weight distribution). For emulsion polymerization, as the surfactant concentration was increased, there was a transition from homogenous to micellar nucleation near the CMC, then a drop in nucleation rate at high surfactant concentration due to insufficient radical flux to support more nucleation. For miniemulsion polymerization, a slow rate of growth of (droplet) nucleation with surfactant concentration was found, followed (at the CMC) by an increase in the rate of nucleation with added surfactant as the mode of nucleation switched to micellar. The conversion-time kinetics of microsuspensions could be modeled with a bulk polymerization model. IOA is sufficiently insoluble in the aqueous phase that emulsion polymerization may or may not be reaction limited. The presence of a stabilizer such a PAA, the use of an oil-soluble initiator such as BPO, and the insolubility of IOA in the aqueous phase all push the polymerization locus toward droplet (microsuspension) nucleation and bulk kinetics. © 2006 Wiley Periodicals, Inc. J Appl Polym Sci 102: 5649–5666, 2006

Key words: polymerization; emulsion; isooctyl acrylate; microsuspension

INTRODUCTION

In the field of dispersed-phase polymerization, certain reaction routes and starting materials are frequently associated with one another. Monomers that display some degree of water solubility, such as styrene and vinyl acetate, are regarded as good candidates for emulsion polymerization. Water-soluble initiators are most often used with systems of this type. When the monomer is very much less miscible with water, suspension polymerization is the alternative most often employed; species such as long-chain acrylates fall into this category. In these cases, initiators that readily dissolve in the organic phase (the ''oil'') are usually used.

While such generalizations may be useful, they fail to take into account the many factors that can affect the dominant polymerization route in a given system. Replacing an ionic (water-soluble) initiator with a nonionic, oil-soluble one encourages bulk polymerization kinetics even when the monomer can diffuse through the aqueous phase, for example. Conversely, if a hydrophobic monomer can be made to diffuse quickly enough to feed a growing chain, the end result will be a proliferation of emulsion polymer particles. Needless to say, the possible combinations of additives and recipe modifications vary greatly, as do the effects they can have on a particular system.

A consideration of the details of each type of reaction is in order. In suspension polymerization, the monomer droplets are typically very large, on the order of hundreds of microns, and may have a layer of stabilizer molecules at their surface. This is a compound, usually water-soluble, that helps to retard coagulation of the particles during reaction. They may work by increasing the aqueous-phase viscosity, creating steric hindrance to coagulation, providing electrostatic repulsion between particles (if the stabilizer is ionic), or some combination of these methods. A distinction must be drawn between true suspensions, whose recipes are as described above, and microsuspensions, which typically contain a significant amount of surfactant as well. Smaller droplets can thus be formed under such conditions. Depending on the water solubilities of the other components, it may be possible to produce submicron particles similar to those that would be obtained in an emulsion. In microsuspension polymerization, the (oil-soluble) initiator is dissolved in the organic phase, giving the possibility of large numbers of radicals per particle (droplet). As a result, the polymerization proceeds as if it were a bulk reaction being run in many tiny reactors. Particles from a suspension

Correspondence to: F. J. Schork (joseph.schork@chbe.gatech.edu).

polymerization are generally in the 10–1000 μm range, and perhaps an order of magnitude smaller in a microsuspension. In its simplest form, emulsion polymerization involves nucleation of surfactant micelles to form submicron particles. The very large (10 μm) monomer droplets act simply as *in situ* feed tanks, supplying monomer to the polymerizing polymer particles via diffusion. Polymer particles produced in an emulsion are usually smaller than 1 μm. (Microsuspension systems will sometimes produce a small quantity of emulsion polymer. This can impact colloidal stability and molecular weight distribution.) Miniemulsion polymerization involves the reduction of the monomer droplets to substantially below 1 μm by the use of high shear and a surfactant/costabilizer system. Nucleation and polymerization take place in submicron polymer particles derived from the monomer droplets. Diffusion across the aqueous phase is minimized.

It can be seen then, that suspension, microsuspension and miniemulsion polymerization require little or no monomer diffusion across the aqueous phase, while emulsion polymerization requires this diffusional process. (However, if a water-soluble initiator is used, then some water solubility of the monomer is required in order for very short oligomers to be formed in the aqueous phase, giving the radical species sufficient surface activity to be absorbed into a monomer droplet; this is true for emulsion polymerization as well.) For a highly water-insoluble monomer, relatively slow monomer transport across the aqueous phase may impact the mechanism of polymerization and polymer structure. In emulsion and miniemulsion polymerization, the loci of polymerization are small particles in which the number of live radicals at any given time is small, while in both microsuspensions and suspensions, the number of radicals per particle is high enough to assume mass action (bulk) kinetics hold. The goal of this paper is to investigate the mass transfer and radical flux phenomena at work in dispersed-phase polymerization of a relatively water-insoluble monomer, isooctyl acrylate (IOA), using water- and oil-soluble initiators in three polymerization systems: emulsion, miniemulsion, and microsuspension. This monomer was selected due to its hydrophobic nature and low glass transition temperature (ca. −45 to −65°C).[1] The question of chain mobility and its effect on final properties can be explored, since the polymer will be in its amorphous state throughout the entire reaction.

THEORY

Bulk polymerization kinetics

Suspension (and microsuspension) polymerization is relatively easy to characterize from a kinetic point of view, particularly when certain simplifying assumptions are justified. Rodriguez[2] provides the following description of the mechanism:

1. Thermal decomposition of initiator

$$I_2 \xrightarrow{k_2} 2I^*$$

2. Rapid one-step propagation

$$I^* + M \xrightarrow{k_2} M^*$$

3. Chain propagation

$$M_n^* + M \xrightarrow{k_2} M_{n+1}^* \qquad (n \geq 1)$$

4. Termination (coupling or disproportionation)

$$M_n^* + M_m^* \xrightarrow{K_{11}} P_{n+m}$$

$$M_n^* + M_m^* \xrightarrow{K_{12}} P_n + P_m$$

P represents a dead polymer chain. The two rate constants in Step 4 are frequently lumped together into a single k_t value for simplicity. A fifth step can also occur[2]:

5. Chain transfer to monomer and polymer

$$M_n^* + M \xrightarrow{k_M} P_n + M^*$$

$$M_n^* + P_m \xrightarrow{k_p} P_n + M_m^*$$

Assuming that the new radical is as reactive as those generated from Step 2, the kinetics of monomer consumption are unaffected by chain transfer; only the molecular weight will change. Transfer to monomer will lower the number average M_n, while transfer to polymer (branching) will raise the weight average M_w and leave M_n unchanged. If this latter process occurs frequently enough, it is possible to produce molecules of extremely high weight and/or extensive branching.

If steady states are assumed for the radical concentrations, and the propagation step consumes essentially all the monomer that reacts, the following expression is obtained for the conversion, x:[2]

$$\ln \frac{[M]}{[M]_o} = \ln (1 - x) = -k_p \left(\frac{f k_d}{k_t}\right)^{0.5} [I]_o^{0.5} t \qquad (1)$$

In the above equation, f is the initiator efficiency factor. The above is exact only if the monomer and polymer densities are equal, but if the two differ by only a few percent, it is still a good approximation.

As the conversion rises, the viscosity within the particles increases dramatically. Diffusion of molecules in the organic phase is thus greatly hindered; newly formed initiator radicals may not be able to move far enough away from one another on the time scale for recombination. The effect is to reduce the total number of active radicals and thus retard further polymerization (the ''cage effect'' observed in many microsuspensions).

If the particle size in a microsuspension approaches that of an emulsion or miniemulsion, the kinetics may be the segregated kinetics discussed below.

Emulsion polymerization

In the classical theory proposed by Flory,[3] an emulsion polymerization can be divided into three intervals. At the beginning, monomer is present as large droplets that are partially or totally covered with a layer of surfactant molecules. Additional surfactant is present in the aqueous phase as either free molecules or micelles; the latter are present only if the critical micelle concentration (CMC) has been exceeded. During Interval I, micelles swollen with monomer capture initiator radicals that have propagated to a critical chain length in the aqueous phase. These newly nucleated particles grow by diffusion of monomer from the droplets and must adsorb more surfactant to stabilize the additional surface area thus formed. Interval II starts when the micelles have been consumed, either by being nucleated to form particles, or by disappearing to supply surfactant to the growing interfacial area of the exiting particles. This point marks the end of primary nucleation. A roughly constant polymerization rate is established as monomer continues to diffuse from the droplets and across the aqueous phase. The rate R_p is given by[2]

$$R_p = \frac{k_p[M]_p \mathrm{n} N_p}{N_A} \tag{2}$$

where N_p is the particle number, $[M]_p$ is the monomer concentration within the particles, and k_p is the propagation rate constant, N_A is Avogadro's Number, and [mac]n is the average number of radicals per particle. Deviations from this model are not uncommon. Ghielmi and coworkers state that if [mac]n is very small (say, 0.01), the probability of a new radical entering a particle that already has one is very small. Hence, termination by coupling can be ignored and the system can be modeled as a bulk polymerization in which the radical concentration is equal to that in the particles. According to the authors, the frequency of radical exit from the particles must be high and the initiation rate low to achieve this situation.[4]

At the other extreme is the pseudobulk system, in which [mac]n is higher than 0.5. If termination is assumed to be independent of chain length, [mac]n varies with time according to eq. (3), which includes the conventional termination constant and the swollen particle volume.[5]

$$\frac{d\mathrm{n}}{dt} = \rho - k\mathrm{n} - \frac{2k(\mathrm{n})^2}{N_A V_s} \tag{3}$$

The constants ρ and k are pseudofirst-order rate coefficients for entry and exit of radicals, respectively, while the last term models second order termination within the particles. Here, it is assumed that the radicals are spread among the particles according to a Poisson distribution—justified when [mac]n is large.[6] Gilbert points out that this pseudobulk equation is not necessarily limited to that particular situation, though. Under certain circumstances, it can be applied when [mac]n is small, even less than 0.5. It has been shown that the fully compartmentalized Smith–Ewart model can predict the same results as the pseudobulk one if [mac]$n \geq 0.7$, and that the two models perform identically unless ρ and k are both less than $(k_t/N_A V_s)$.[7]

Given the propagation rate constant k_p, a generalized formula for monomer conversion (x) during the course of an emulsion polymerization is this[7]:

$$\frac{dx}{dt} = \frac{k_p[M]_p N_c}{n_M^o N_A}\mathrm{n} \tag{4}$$

N_c and n_M^o are the number of particles and initial moles of monomer per volume of aqueous phase (not total latex), respectively. This expression is valid through Intervals I and II, with $[M]_p$ being essentially constant in Interval II.

Interval III begins when the monomer droplets disappear. At this point, the monomer concentration within the particles begins to decrease, as there are no more droplets to feed them via diffusion. As the reaction starts to resemble a bulk polymerization at this point, the conversion can be recast to account for this fact. If $[M]_{\mathrm{po}}$ is the concentration at the start of Interval III, $[M]_p$ during Interval III may be written as

$$[M]_p = (I - x_{\mathrm{conc}})[M]_{Po} \tag{5}$$

where

$$x_{\mathrm{conc}} = \frac{(x - x_{\mathrm{III}})}{(I - x_{\mathrm{III}})} \tag{6}$$

and x_{III} is the monomer conversion at the beginning of Interval III. Substituting eq. (5) into eq. (4) and

TABLE I
Data on Propagation Kinetics: Acrylates and Methacrylates (From Ref. 8)

Monomer	T (°C)	k_p (L/mol s)	$\log_{10}k_p$	E_p (kJ/mol)	$\log_{10}A$
n-Butyl acrylate	50	2800	3.45	17.4	6.26
n-Butyl acrylate	20	1400	3.15	17.4	6.26
n-Butyl methacrylate	50	790	2.90	21.8	6.39
2-Ethylhexyl acrylate	20	1700	3.23	–	–
2-Ethylhexyl methacrylate	50	940	2.97	20.4	6.27
n-Dodecyl acrylate	20	1900	3.28	–	–
n-Dodecyl methacrylate	50	1010	3.00	20.8	6.37

replacing n_M° with n_M^{III} to reflect all conditions at the beginning of Interval III, the conversion profile is given as[7]

$$\frac{-d\,\ln(1-x_{\mathrm{conc}})}{dt} = \frac{k_p[M]_{po}N_c}{n_M^{III}N_A}\mathrm{n} \tag{7}$$

Miniemulsion polymerization

In a miniemulsion system, a combination of high shear and an effective surfactant/cosurfactant system is used to reduce the monomer droplet size to the submicron range. The surfactant provides stability of the droplets against coalescence. The costabilizer (commonly a hydrocarbon such as hexadecane, or a long-chain alcohol such as cetyl alcohol) is used to limit Ostwald ripening. Ostwald ripening is the diffusion of monomer from the small droplets to the larges ones, thus reducing the overall interfacial area of the system. Waterborne radicals, therefore tend to be selectively captured by the droplets, and propagation takes place in the resulting particles, with little or no monomer transport. (Note: if some droplets are nucleated, while others are not, the diffusion from the droplets/particles containing little polymer and those containing higher levels of polymer will occur. Zero monomer transport is only achieved in the idea.) However, the polymer particles formed during miniemulsion polymerization are sufficiently small that the bulk kinetics seen in suspension and microsuspension are not necessarily found in these systems.

Many of the equations described previously for emulsions do not apply in their given form for miniemulsions. First, the particle number becomes a complex function of both surfactant level and the energy used to break the organic phase into the small droplets. Second, eq. (2) is applicable if one understands that the monomer concentration within particles, which will not be constant; there is no outside source to keep feeding them. The system starts to resemble Interval III of Smith–Ewart kinetics once the particles are nucleated. Equation (7) therefore becomes more appropriate, and if [mac]n is small, the kinetics revert to the bulk model.

Estimation of properties reaction rate constant

In his study of emulsion polymerization using extremely hydrophobic monomers, Balic collected data for the kinetics of a number of acrylates and methacrylates,[8] shown in Table I. These can be used to estimate of the k_p values for IOA. In this table, E_p and A are the Arrhenius parameters. Correcting all data to other temperatures and comparing monomers with identical alkyl groups yields the results in Table II.

The relative insensitivity of methacrylate/acrylate k_p ratios to alkyl group size (C-4–C-12) at 20°C suggests that the same condition will hold at other temperatures if a reliable estimate of the methacrylate coefficients can be found. The average of the 20°C ratios is 0.246, which can be taken as a representative value for *n*-BMA (C-4). Fitting a line to this point and the ones at 30°C and 50°C gives the following relation:

$$k_p(\mathrm{methacr})/k_p(\mathrm{acr}) = 0.6268 - 111.48/T(K); R^2 = 0.997 \tag{8}$$

The isooctyl group is nearly identical to the 2-ethylhexyl, so it is not unreasonable to assume that the isooctyl acrylate and 2-ethylhexyl acrylate will have

TABLE II
Propagation Coefficients from Table I, Corrected to Other Temperatures

Monomer	T (°C)	k_p (L/mol s)	$\log_{10}k_p$	k_p(methacr)/k_p(acr)
n-BA	30	1770	3.25	–
n-BMA	20	340	2.53	0.243
n-BMA	30	460	2.66	0.260
n-BMA	50	790	2.90	0.282
2-EHMA	20	430	2.63	0.253
2-EHMA	30	570	2.75	–
2-EHMA	60	1180	3.07	–
n-DDMA	20	460	2.66	0.242
n-DDMA	30	610	2.79	–

TABLE III
Estimated Acrylate Propagation Coefficients at Reaction Temperatures

Monomer	T (°C)	k_p(methacr)/k_p(acr)	k_p (L/mol s)
IOA	50	0.282	3330
IOA	60	0.292	4040

roughly the same reactivity at 60°C, the temperature reported for the latter monomer in Table II. Using the 2-ethylhexyl methacrylate data at 50°C results in

$$\log_{10} k_p(\text{methacr, } 50^{\circ}\text{C}) = 2.8567 + 0.0125(\#\ \text{carbons}); R^2 = 0.949 \quad (9)$$

Now all the desired values can be estimated using the preceding data and regressions; the results are given in Table III. Because of the number of assumptions inherent in this estimate it is not possible to put an accurate error estimate on the data in Table III; they should be considered only as order-of-magnitude estimates.

EXPERIMENTAL

Reagents

IOA was first treated to remove the hydroquinone monomethyl ether that had been added by the manufacturer to inhibit polymerization. An aqueous wash solution of 10 wt % sodium hydroxide, saturated with sodium chloride, was mixed with the monomer and subjected to magnetic stirring for 30 min. The volume ratio of monomer to solution was approximately 5 : 1. The mixture was then poured into a separatory funnel and left standing overnight to allow the phases to split; the aqueous phase was discarded and the monomer treated with a few grams of calcium sulfate to remove any residual water. Finally, the solids were removed by vacuum filtration.

Poly(acrylic acid), or PAA ($M_w \sim 250{,}000$), was delivered as a solution of ~35 wt % in water. Before use, it was diluted to 15% to reduce the viscosity and provide for easier handling. Ammonium hydroxide, hexadecane (HD), sodium lauryl sulfate (SLS), potassium persulfate (KPS), and benzoyl peroxide BPO) were used as delivered. The NH_4OH was supplied by Fisher Scientific (Hampton, NH), while all other components were delivered by Aldrich-Aldrich (St. Louis, MO). Tables IV–VII give the details of all recipes used in this work.

Reaction apparatus

For all experiments, a 500-mL batch reactor, fitted with stirring motor and water-cooled condenser, was used. The vessel was heated by a thermostat-controlled water bath and could be purged with nitrogen as needed.

Emulsion polymerization

To prepare the equipment, the reactor was assembled and the water bath heater was started with a setpoint of 50°C. The nitrogen purge was started at high speed (~3–4 mL/s) to allow ample time for the oxygen to be flushed out; at the same time, the stirrer was activated at a speed of 300 rpm and the condenser cooling water was started.

The required quantity of water was weighed out and a small quantity set aside for later use with the KPS. Next, the required amount of SLS was added to the bulk of the water and allowed to dissolve. The monomer charge was then added to the solution and stirred magnetically for 30 min. By the end of this time, the reactor had been purging for at least 60 min and the water bath was up to the desired temperature. The batch was then loaded in and put under fast purge for 2–3 min to remove any oxygen that had entered in this step. Next the nitrogen was slowed and the reactor left to equilibrate for 30 min.

Near the end of this time, the required KPS was dissolved in the water that had been set aside. This solution was injected into the reactor to mark the start of the polymerization. For the next 120 min, samples were withdrawn at 10-min intervals and mixed with preweighed amounts of cold hydroquinone solution (0.5 wt % in water) to short-stop the reaction.

When PAA was used, the water was reduced by a few grams to account for that contained in the stock and a small portion was removed for the KPS. The PAA was added to the remaining water and then neutralized to pH 7 with concentrated NH_4OH. The SLS was then added and the remainder of the procedure was followed as above.

Miniemulsion polymerization

The miniemulsion experiments were set up according to the same procedure as their emulsion counter-

TABLE IV
Recipes for Emulsion Polymerization of IOA using KPS

Run #	H_2O (g)	IOA (g)	KPS (mmol/L)	SLS (mmol/L)
1	272.79	94.76	9.963	4.984
2	272.29	94.47	10.001	6.487
3	272.01	95.34	9.989	7.989
4	275.26	95.45	9.874	9.882
5	272.52	95.33	9.973	12.981
6	272.30	94.71	9.985	14.967
7	272.20	94.85	10.004	19.883
8	272.07	95.28	10.006	24.992

All reactions carried out at 50°C and 300 rpm stirring.

TABLE V
Recipes for Emulsion Polymerization of IOA, using KPS and PAA Stabilizer

Run #	Total H_2O (g)	IOA (g)	KPS (mmol/L)	SLS (mmol/L)	PAA (g solids)
1	272.19	95.43	9.981	2.989	0.768
2	271.98	95.04	10.011	4.990	0.767
3	272.00	94.65	10.006	8.005	0.771
4	271.99	94.95	9.995	9.990	0.767
5	271.80	95.08	10.027	13.014	0.772
6	272.11	94.87	9.995	14.994	0.769
7	271.96	94.97	10.012	20.006	0.771
8	272.09	94.49	9.997	24.987	0.774

All reactions were carried out at 50°C and 300 rpm stirring.

parts, with the following changes. Before stirring began, HD was added to the monomer phase to give a 50 : 1 weight ratio of the latter to the former. Stirring lasted for 60 min, after which the batch was sonicated with a Fisher Model 300 Sonic Dismembrator, set to 70% relative output, for 20 min. This equipment generated a significant amount of heat in the mixture, but preliminary tests revealed that the temperature rise did not cause polymerization to start in the absence of initiator. Therefore, no cooling bath was used during the sonication; however, the container was covered to minimize liquid loss from evaporation.

Microsuspension polymerization

In the IOA microsuspensions, no water was set aside for dissolving initiator; the amount was still reduced slightly to account for the PAA stock. The acid was added, followed by NH_4OH and SLS. The ratio of SLS to PAA was taken from Baker and Ketola[9] to provide stability of particles in the tens of micron range; no effort was made to optimize this ratio. BPO was then mixed into the monomer to match the concentration used by Baker and Ketola[9] (approximately 9 m*M* active initiator), and the phases were stirred together for 30 min. The batch was then charged to the reactor, under nitrogen purge and suspended above the water bath so as to keep the initiator from dissociating prematurely. After the 30-min equilibration, the vessel was lowered into the bath, which was maintained at 60°C, and allowed to heat for 25 min before the first sample was taken. Four others were drawn at 10-min intervals after this point, then five more every 15 min. The total reaction time after lowering the reactor was thus 140 min.

Sample analysis

To determine the degree of conversion gravimetrically, small amounts of the samples were measured into preweighed pans and dried in an oven overnight at 70–90°C. The resulting solids content was corrected for nonvolatile salts and additives to find the actual polymer formed. Although IOA has a very high boiling point (~125°C at 15 mmHg), the drying temperatures were found to be sufficient to drive off the unreacted material after one night. This observation was confirmed by subjecting a small quantity of the washed monomer to the same conditions. The next morning, the liquid had completely evaporated and there was no solid residue, indicating that thermal generation of free radicals was not taking place to cause polymer to form in the oven.

Molecular weights were determined by gel permeation chromatography (GPC) using two columns. The first (Phenomenex) had a pore size of 10^3 Å, while the second (Viscotek) was a mixed-bed column designed to give a linear calibration. However, it was found that putting the small-pore column in front gave better accuracy with known standards. A Waters 410 differential refractometer and Viscotek T60A detector provided data to the TriSEC 3.0 software (Viscotek). Tetrahydrofuran (THF) was used both as eluent and as solvent for the samples; solutions were made up to overall concentrations of 3–8 mg polymer/mL liquid. These were then filtered to remove any insoluble material and then injected into the system, passing through a second filter before entering the columns and detector. Poly(methyl methacrylate) standards were used for the calibration, with the molecular weights of these being

TABLE VI
Recipes for Miniemulsion Polymerization of IOA, using KPS

Run #	H_2O (g)	IOA (g)	KPS (mmol/L)	SLS (mmol/L)	HD (g)
1	272.32	95.48	9.986	2.991	1.92
2	272.45	95.35	9.996	7.976	1.96
3	272.40	94.47	9.978	9.983	1.95
4	272.03	95.69	9.999	12.982	1.95
5	272.33	95.33	9.980	14.973	1.96
6	272.19	94.66	9.987	19.965	1.96
7	272.49	95.00	9.974	24.949	1.94

All reactions were carried out at 50°C and 300 rpm stirring.

TABLE VII
Recipes for Microsuspension Polymerization of IOA, using BPO as Initiator

Run #	Total H_2O (g)	IOA (g)	BPO (mmol/L)	SLS (mmol/L)	PAA (g solids)
1	271.93	95.03	8.942	4.950	0.772
2	271.94	94.87	8.957	7.407	0.770
3	272.17	94.66	8.919	9.597	0.787
4	272.13	94.82	8.908	14.839	0.772
5	271.75	95.25	8.875	19.811	0.773
6	271.92	94.81	8.936	24.727	0.773

All reactions were carried out at 60°C and 400 rpm stirring.

corrected for the polymers formed in this work. Assuming that the columns perform their separation based on hydrodynamic volume $M[\eta]$ of the polymer molecules, the adjustment is fairly straightforward. The Mark–Houwink–Sakurada equation predicts:

$$[\eta] = KM^a \tag{10}$$

where K and a are parameters that have been tabulated for many polymers. If molecules of equal hydrodynamic volume have the same elution time, then for an unknown and a reference, the following holds:

$$K_{\text{ref}} M_{\text{ref}}^{a\ \text{ref}+1} = \text{KM}^{a+1} \tag{11}$$

Rearranging,

$$M = \left(\frac{K_{\text{ref}}}{K}\right)^{\frac{1}{a+1}} (M_{\text{ref}})^{B\frac{\text{ref}+1}{a+1}} \tag{12}$$

Since exact parameters for poly(IOA) are hard to come by, it is necessary to estimate then based on values for structurally similar materials. Linear regression on MHS parameters for various methacrylate polymers in THF (see Table VIII) and correcting the proportionality constant for the lack of the extra methyl group in the actual polymer yields the following correlation between the standards and poly(IOA):

$$M = 1.1546(M_{\text{ref}})^{0.9885} \tag{13}$$

Equation (13) is only strictly valid for linear polymer; varying levels of branching may introduce some error, but this is not thought to be highly significant. The columns used in this work could only handle standard molecular weights up to 10^7 g/mol. Any GPC signals corresponding to higher weights were assigned to ''gel precursor'' polymer-soluble and therefore not as highly branched as true gel, but not classifiable with the existing equipment.

Particle size distributions were obtained by dynamic light scattering, using a Protein Solutions DynaPro system connected to the company's Model LSR microsampler. A drop of sample was placed in a cuvette and diluted with deionized water, to a volume of roughly 4 mL, or a 100 : 1 volume ratio. This mixture was then diluted further until it gave a count rate that did not exceed the detector's upper limit; in most cases, this entailed another 100 : 1 addition of water. Twenty measurements were taken per sample. For recipes in which both droplet nucleation and micellar nucleation were operative (microsuspension and emulsion with PAA), the particle size distributions were bimodal. The mean of each mode was recorded separately.

Polymer density was determined by dissolving a few grams of a final latex batch in THF and allowing the solution to dry overnight. A small amount of the dried material was then placed in a measured amount of water, and ethanol was added until the sample began to sink. Viscosities of the organic and aqueous phases at the temperatures of interest were measured with a Brookfield RVTDV-1 Digital Viscometer. Monomer density was listed by the manufacturer as 0.880 g/cm^3.

The critical micelle concentration of SLS under the various reaction conditions was found through molar conductivity measurements. A solution with the appropriate additives (PAA, KPS, etc.) was made up and half of it set aside, while sufficient SLS was dissolved in the other half to raise it to approximately ten times the CMC, and this mixture was heated to the desired temperature. The solution without surfactant was added a little at a time, and the conductivity was measured after each step. To determine

TABLE VIII
MHS Parameters for Methacrylate Polymers in THF

Alkyl group	K ($\times 10^3$ mL/g)	a
Methyl	7.50	0.72
Isobornyl	3.68	0.73
Butyl	5.84	0.76
Decyl	4.56	0.73
Tridecyl	4.75	0.71
Octadecyl	2.50	0.75
Isooctyl	5.14	0.74

The last value, for isooctyl (C-8), is calculated from linear regression on the others, which are taken from Ref. 1.

TABLE IX
Experimental Data for IOA Emulsion Polymerization with KPS

Run #	Sample time (min)	M_n ($\times 10^{-3}$ g/mol)	M_w ($\times 10^{-3}$ g/mol)	% pseudogel	Unswollen particle radius (nm)
5	20	111.7	1779	6.8	41.62
	30	159.8	1934	39.9	50.32
	40	88.4	1833	46.6	40.98
	50	124.7	1883	49.7	49.63
	60	130.2	1781	50.4	48.44
	90	101.9	1730	50.9	50.71
	120	76.6	1711	47.8	51.20
6	20	274.5	2448	24.4	44.53
	30	324.5	1871	56.0	48.63
	40	329.6	1834	58.2	50.48
	50	321.1	1739	61.7	53.14
	60	311.3	1655	60.7	50.66
	100	289.7	1614	61.6	49.78
7	10	107.1	779	0.55	
	20	172.2	2345	49.2	48.48
	30	125.7	2086	54.5	47.82
	40	263.0	2268	47.3	50.48
	60	114.7	1998	54.4	50.33
	80	153.2	2087	60.9	48.39
	110	111.2	2017	58.2	48.10
8	20	180.5	2450	49.6	44.57
	30	185.3	2223	59.8	45.72
	40	142.3	1875	58.4	45.56
	50	128.5	2059	59.5	46.33
	70	116.1	2024	59.2	47.03
	100	107.5	1964	59.5	45.76

the CMC, molar conductivity (meter reading divided by SLS concentration) was plotted and fitted to a piecewise linear model to pinpoint the discontinuity in the values, using the squared residuals as the criterion.

RESULTS AND DISCUSSION

The polymer density was calculated as 0.916 g/cm^3, based on the mass fraction of ethanol needed to make the solid sample begin to sink (47.4% in water) and using solution properties given by Perry[10] Vanderhoff[11] has reported the water solubility of IOA as 62 ppm, or 0.34 m*M*. Vinyl neodecanoate, investigated by Balic,[8] has a much lower solubility of 0.038 m*M*. The question of whether species as hydrophobic as this can reasonably be expected to follow Smith–Ewart kinetics will be addressed shortly.

Emulsion and miniemulsion kinetics

Conversion, molecular weight, and particle size results for all samples are given in Table IX and X, and in Figures 1–3. Both the emulsion and miniemulsion runs show increasing rate of conversion with increasing surfactant concentration (although the mechanism of particle nucleation is quite different). Final particle concentrations (number per unit volume of water) for emulsions and miniemulsions were calculated based on the properties of the last sample for a run, using the relation:

$$N_{c,f} = \frac{X_f m_M}{\frac{4}{3}\pi(r)^3 V_W d_p} \tag{14}$$

The formula calculates the total volume of polymer (mass converted over density) and the volume of a single particle. Based on the small volume of actual latex and high dilution ratio used for the size measurement, essentially all the unreacted monomer was stripped out of the particles. The values in Table IX and X are therefore the unswollen radii.

Log–log plots of N_c versus [SLS] in the emulsions and miniemulsions are shown in Figure 4. It is apparent from these graphs that there is a marked discontinuity in each set. Piecewise linear regression on the data points, with the break point chosen to minimize the total residuals are shown. It can be seen from these results that the break in the particle numbers generally corresponds well with the CMC as

TABLE X
Experimental Data for IOA Miniemulsion Polymerization with KPS

Run #	Sample time (min)	M_n ($\times 10^{-3}$ g/mol)	M_w ($\times 10^{-3}$ g/mol)	% pseudogel	Unswollen particle radius (nm)
1	20	149.4	1897	11.1	101.27
	30	114.6	1788	27.2	95.94
	40	86.1	1580	49.1	99.93
	50	84.5	1593	56.6	97.28
	60	75.1	1406	65.2	101.49
	90	96.3	1409	69.2	102.66
	120	61.4	1125	75.6	99.09
2	30	115.9	1881	15.5	89.06
	40	77.6	1720	23.1	87.71
	50	78.6	1741	39.6	85.04
	60	59.6	1662	47.3	81.39
	80	65.6	1607	52.6	83.54
	100	63.1	1575	51.0	81.92
	120	75.7	1512	58.0	78.95
3	30	441.3	2251	8.2	87.62
	40	421.4	2095	32.1	81.07
	50	106.1	1979	46.9	79.97
	60	118.0	1877	47.3	77.57
	70	102.4	1778	41.0	79.17
	90	92.9	1857	43.8	
	110	84.0	1751	43.4	77.85
4	20	84.3	1564	24.9	79.87
	30	85.2	1726	41.5	82.37
	40	102.4	1790	46.7	79.93
	50	86.0	1732	45.0	78.13
	80	69.6	1669	46.0	74.77
	120	63.2	1663	36.1	75.22

determined from conductivity measurements (Emulsions: CMC = 7.8 m*M*, [SLS] at transition = 10.7 m*M*. Miniemulsions: CMC = 7.8 m*M*, [SLS] at transition = 9.7 m*M*). One trend that immediately becomes apparent is the behavior of the emulsion particle numbers as opposed to those of the miniemulsions. The emulsion particle number trends show a drop in slope after the CMC, while the miniemulsion fit shows an increase in slope. This can be explained in light of data on the particle number as a function of surfactant level, as reported by Vanderhoff[12] in his survey of emulsion polymerization. Such a curve typically describes a sigmoid, with the point of inflection near the CMC. Nucleation at low surfactant concentration was ascribed to homogenous nucleation. Near the CMC, the rapid rise in number of particles was ascribed to micellar nucleation. The low rate of increase in particle number with surfactant concentration was ascribed to radical flux insufficient to nucleate a larger fraction of the micelles. Here, the emulsions exhibit behavior consistent with the upper portion of the curve: a sharp rise near the CMC, then a leveling off. On the other hand, the miniemulsions match the lower portion: more level particle numbers at low surfactant concentrations, then a rise past the break point. The miniemulsions exhibit behavior similar to the low surfactant end of the sigmoid, but the mechanism is very different. Here, the lower slope line corresponds to droplet nucleation rather than to homogenous nucleation, which is not likely to be significant for a monomer of such low water solubility. The steeper slope of the high surfactant line is likely due to micellar nucleation. The transition point for the miniemulsions, relative to the emulsions is surprisingly low. Given the high surface area of a miniemulsion, one would expect the transition point for the miniemulsions to be higher.

Microsuspension kinetics

Figure 5 gives the conversion–time curves for the microsuspension polymerizations. As with the emulsion and miniemulsion polymerizations, the rate of polymerization increases with increasing surfactant. Equation (1) may be used to correlate the conversion–time data for a system exhibiting truly bulk kinetics. After performing the logarithmic transformation on the conversion data, linear regressions

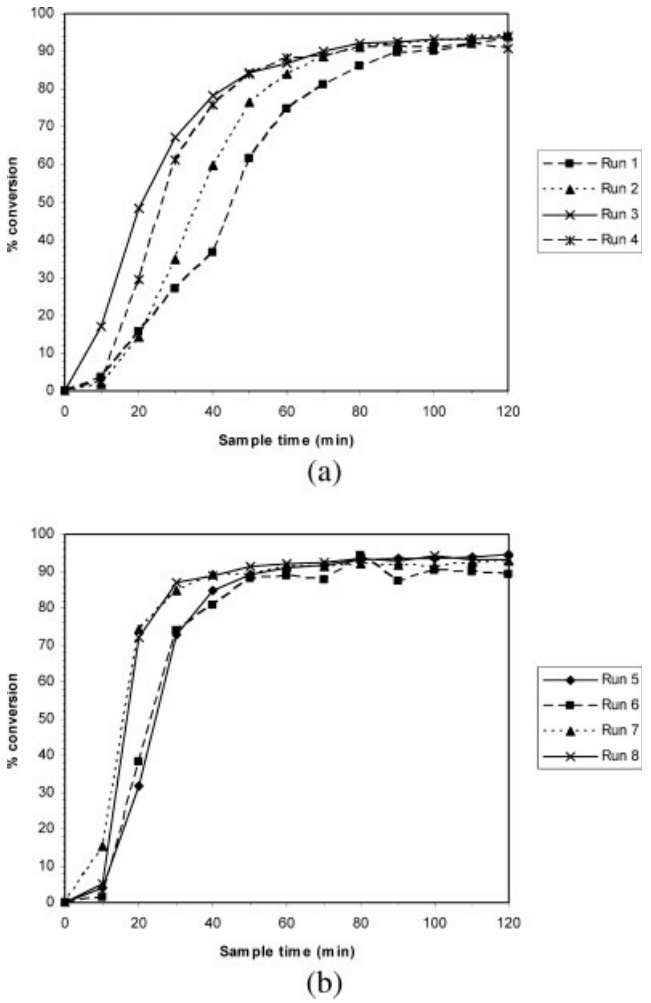

Figure 1 Conversion profiles: IOA emulsions with KPS. (A) low SLS concentrations; (B) high SLS concentrations.

were carried out on the data from the IOA microsuspension runs and optimized by cutting off the later points that strayed noticeably from the line. The results are given in Figures 6–8. The deviation from linearity, starting at about 65–80% conversion, is caused by the onset of the cage effect. To quantify the decrease in the initiator efficiency factor (f), the change in conversion was estimated graphically and used in conjunction with Equation (1) (assuming all other parameters to be constant). Figure 9(A) shows the calculated initiator efficiencies for each run, as a function of time. Figure 9(B) shows the average (over all runs) initiator efficiency correlated with time.

Monomer diffusion considerations in emulsion polymerization of IOA

In the Smith–Ewart description of emulsion polymerization, Interval II relies on the diffusion of monomer to the growing particles from the large droplets. Emulsion polymerization is commonly assumed to be reaction, rather than diffusion limited, but with highly water-insoluble monomer (e.g., IOA), this assumption is worth investigating. Inspection of Figure 1 shows a representative steady-state conversion rate during Interval II of 3% per minute. With a monomer charge of 95 g, this is equal to roughly 0.045 g/s, which is the minimum quantity that would have to be provided by the large droplets in order for the Smith–Ewart theory to be viable.

The starting point for evaluating the situation is to estimate the size of the droplets. During the emulsion experiments, the earliest samples that showed essentially no conversion would separate into two phases within 5 min. The height of the aqueous phase was roughly 3 cm, giving a terminal droplet velocity of 0.01 cm/s. From Stokes' law, this terminal velocity is given for low-Reynolds-number flow as follows:

$$V_{\text{sen}} = \frac{2r^2 g \Delta\rho}{9\mu} \tag{15}$$

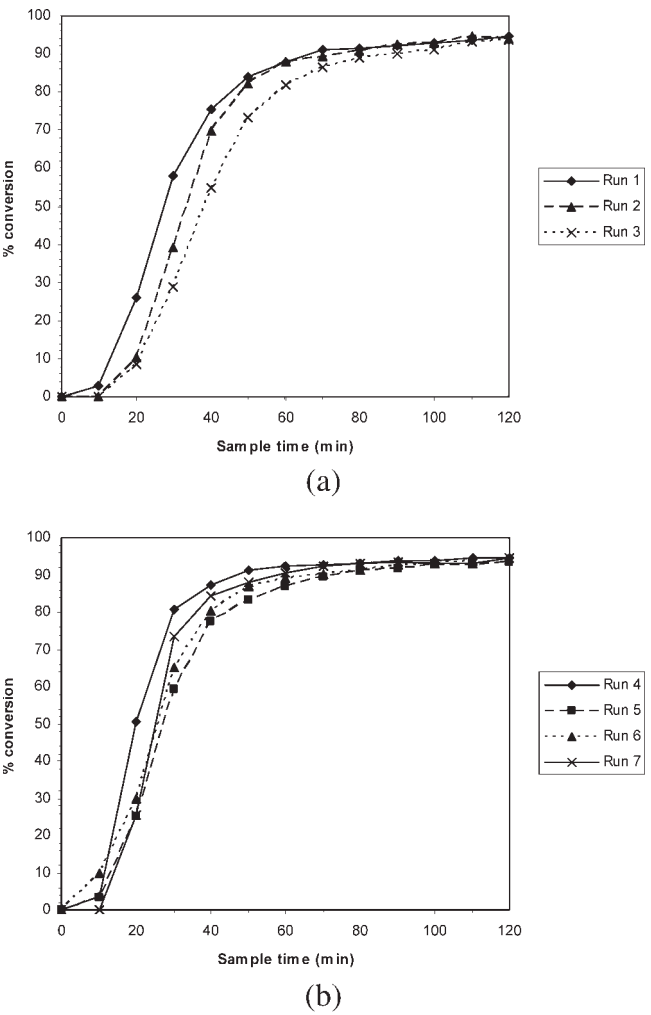

Figure 2 Conversion Profiles: IOA miniemulsions with KPS. (A) low SLS concentrations; (B) high SLS concentrations.

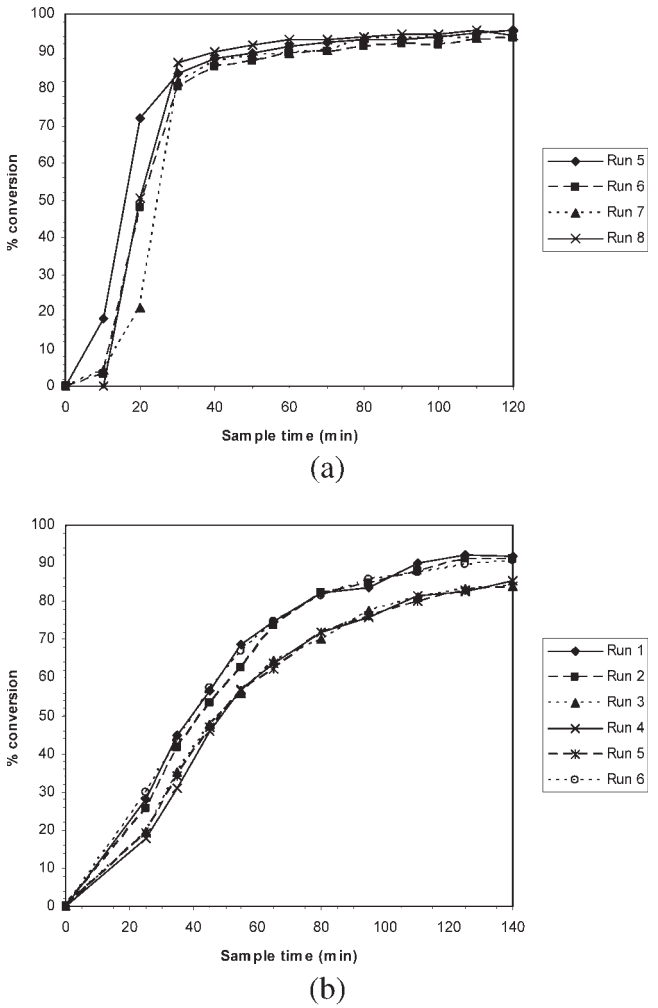

Figure 3 Conversion profiles: IOA emulsions with KPS and PAA. (A) low SLS concentrations; (B) high SLS concentrations.

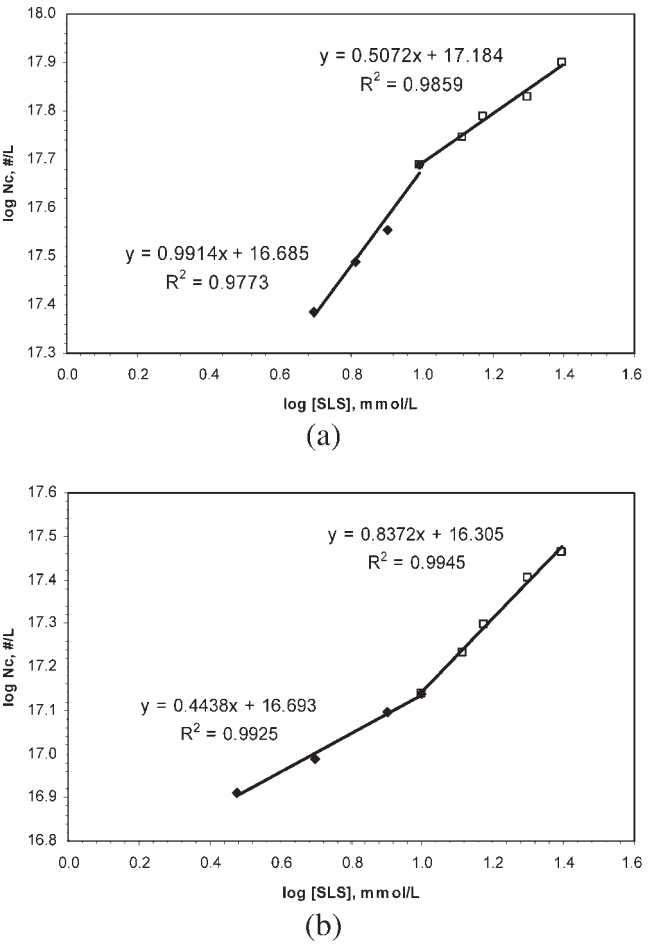

Figure 4 Particle number for IOA polymerization using KPS (no PAA). (A) emulsions; (B) miniemulsions (log[CMC] = 0.9).

In the above, $\Delta\rho$ is the density difference between the droplet and the continuous phase, and g is the acceleration due to gravity. (Equation (15) assumes unhindered settling, which is not likely here, but will be used to provide an approximate measure of the droplet size.) Rearranging the expression and inserting the appropriate physical properties for the water and monomer phases at 50°C results in a droplet radius of 30 μm.

The mass transfer coefficient for monomer leaving the monomer droplets in a similar system has been estimated by Reimers[13] as

$$k_c = \frac{2D_w}{r}. \tag{16}$$

This correlation holds when the droplets are small enough that there is no surface scrubbing, an assumption that is justified for 30-μm droplets. Estimating the diffusivity of IOA in water at 50°C by the Wilke–Chang correlation[13] as 1.46×10^{-5} cm^2/s, the value of k_c can then be estimated as 1×10^{-4} m/s. The

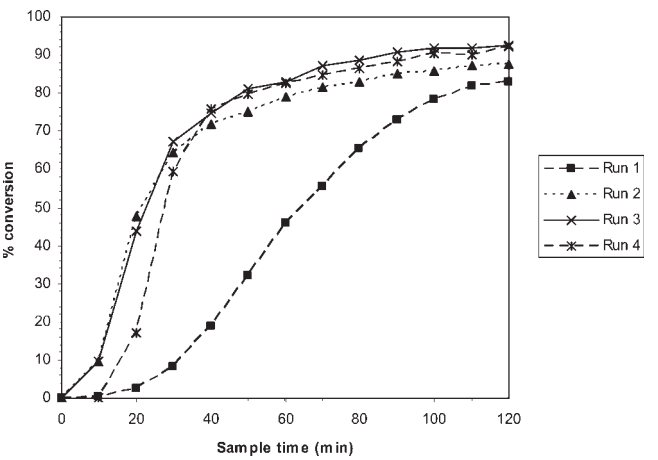

Figure 5 Conversion profiles: IOA microsuspensions with BPO.

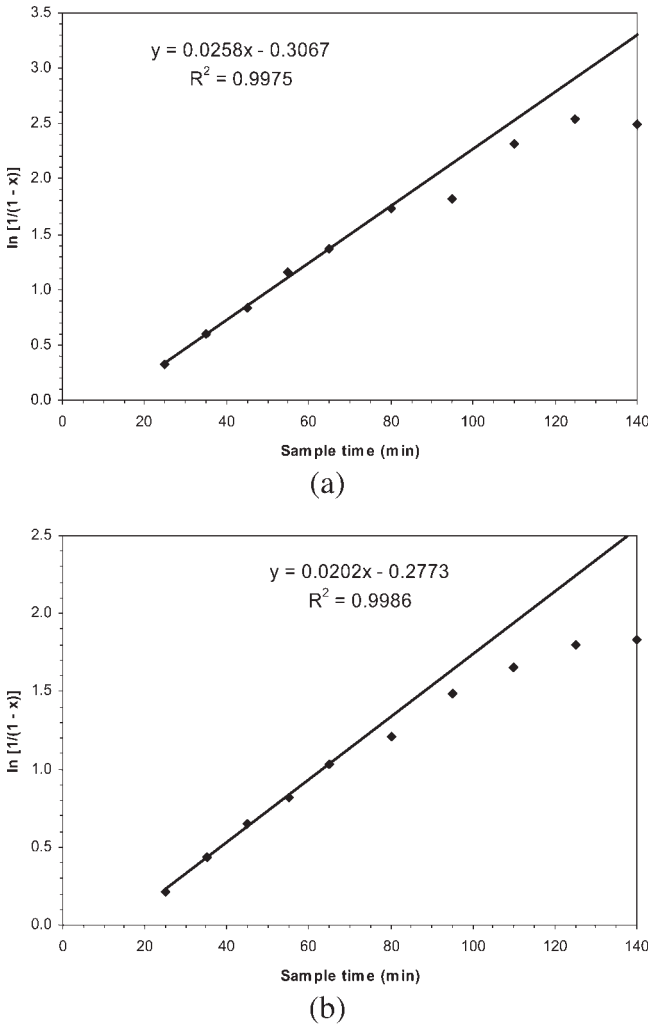

Figure 6 Linear regression of eq. (1) on IOA microsuspension polymerizations. (A) Run 1; (B) Run 2.

maximum mass transfer from the droplets, Q_M, will be given by:

$$Q_M = k_c A_{\text{drop}}([M]_{\text{aq.sat}} - [M]_{\text{aq.bulk}}) \qquad (17)$$

Here, A_{drop} is the total surface area of the droplets per unit volume of aqueous phase. The needed Q_M to support a conversion rate of 3% per minute is 9.0×10^{-4} mol/L s (based on aqueous phase). Using the value of k_c above, the concentration driving force necessary to provide Q_M in the above expression is found to be 2.4×10^{-4} mol/L. The value of the solubility of IOA in water at the reaction temperature is reported as 3.4×10^{-4} mol/L.[19] Thus, to provide a monomer flux of Q_M, the bulk aqueous phase monomer concentration would need to be at less that one-third of the saturation value. All of the above calculations are only order-of-magnitude estimates, but as such, point to the possibility that this system maybe at least partially diffusion, rather than reaction limited. If that is the case, then Smith–Ewart kinetics may not be strictly applicable. It should be noted that similar considerations do not come into play in the miniemulsion polymerizations, since monomer transport in miniemulsions is not critical to the polymerization mechanism.

During the polymerization of the emulsion recipes (excluding the IOA runs with PAA) it was observed that samples would separate into aqueous and large-droplet phases until some point during the quasi-linear portion of the conversion profile. The aqueous phase contained the formed polymer, while the organic phase became less and less prominent until the two merged into a homogeneous mixture. Miniemulsions exhibited a similar behavior, but on a much longer time scale due to the smaller droplet size (~100 nm vs. 20–50 μm); in this case, the aqueous phase was seen to be essentially free of polymer particles which were contained in the upper phase.

In the aqueous phase, new initiator radicals propagate until they reach a critical chain length and

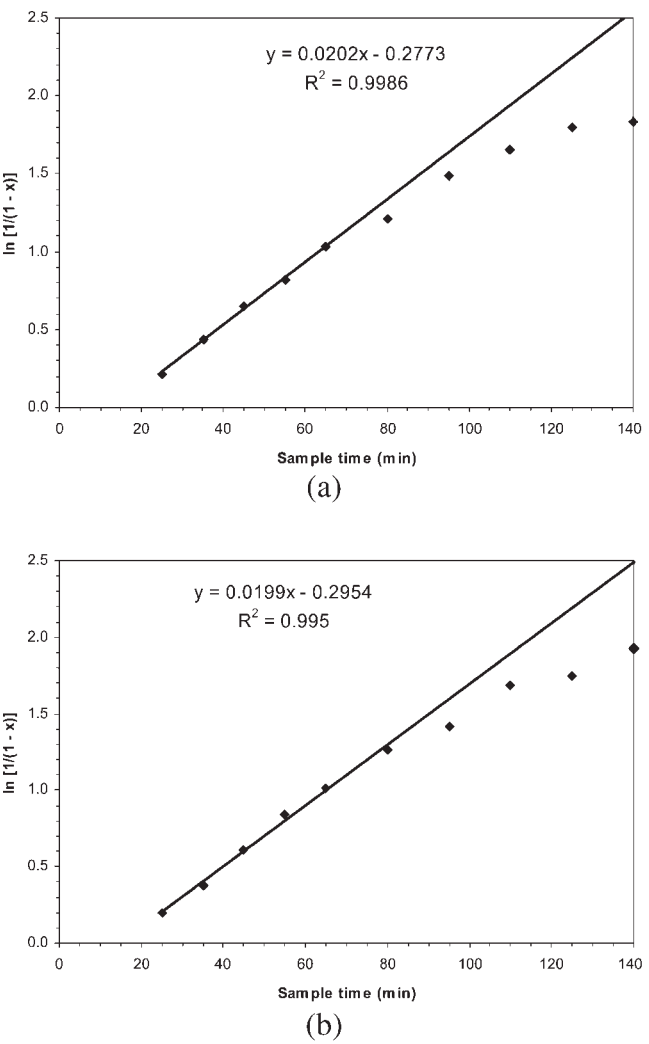

Figure 7 Linear regression of eq. (1) on IOA microsuspension polymerizations. (A) Run 3; (B) Run 4.

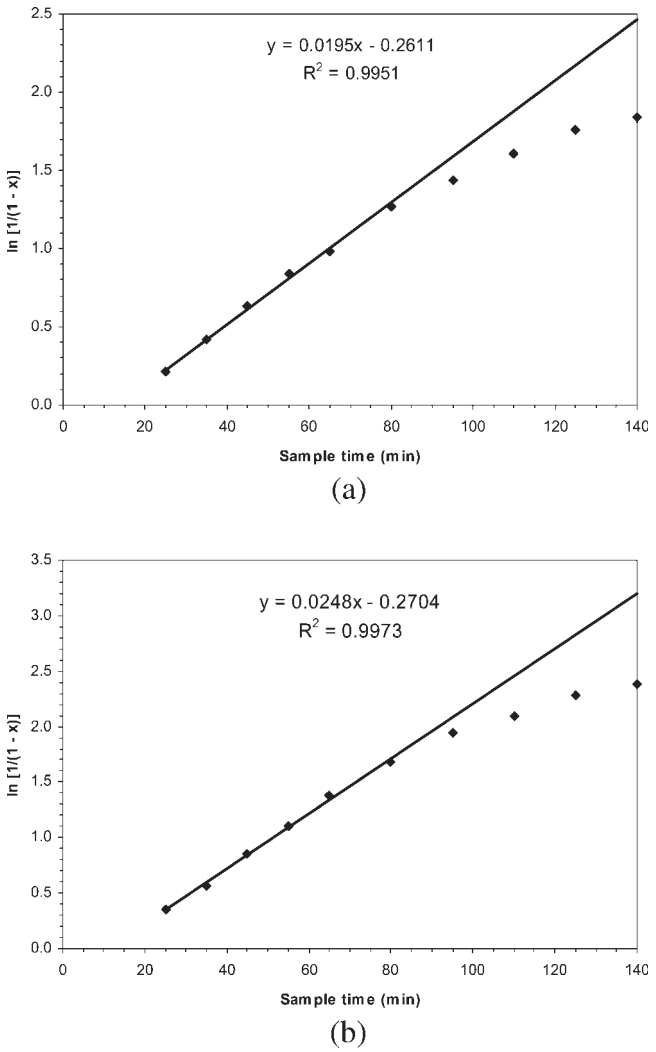

Figure 8 Linear regression of eq. (1) on IOA Microsuspension Polymerizations. (A) Run 5; (B) Run 6.

become too hydrophobic to remain in solution. These can then either terminate with one another or be captured by small droplets or micelles. If termination occurs, a new oligomer is formed, one that has a hydrophilic group on one or both ends (depending on the mode of termination) and several monomer units. Particularly when an ionic initiator such as KPS is used, these oligomers are highly surface active. Wang and Poehlein investigated the issue of critical chain length (for capture into micelles or droplets or particles) in their work with emulsion copolymerization of styrene with more hydrophilic comonomers. When acrylic acid was used, critical lengths of 8–11 units were found, decreasing to 5–6 and 3–4 after methacrylic acid and methyl methacrylate were employed instead, respectively.[14] This marked decrease in length supports the idea that more hydrophobic monomers become capable of being captured after fewer aqueous propagation steps. The fact that IOA is roughly an order of magnitude less soluble than styrene suggests an even shorter critical chain length at work in the systems studied here.

Once polymer particles have been nucleated via oligomeric radical entry into micelles, monomer necessary to sustain polymerization would normally be supplies by monomer diffusion. If diffusion is limited as proposed above, then monomer supply to the particles must be accomplished via a collision mechanism in which particles absorb monomer from monomer droplets. Limitations on monomer transport might favor polymerization in monomer droplets, but given the observed (submicron) particles sizes, this is not likely to be the dominant mechanism of polymerization. This mechanism is similar to the one proposed by Zerfa and Brooks for transfer of radicals from one droplet to another by collision in suspension polymerization reactions.[15]

Droplet versus micellar nucleation

Two different recipes have been employed to study the formation of large particles in IOA dispersions.

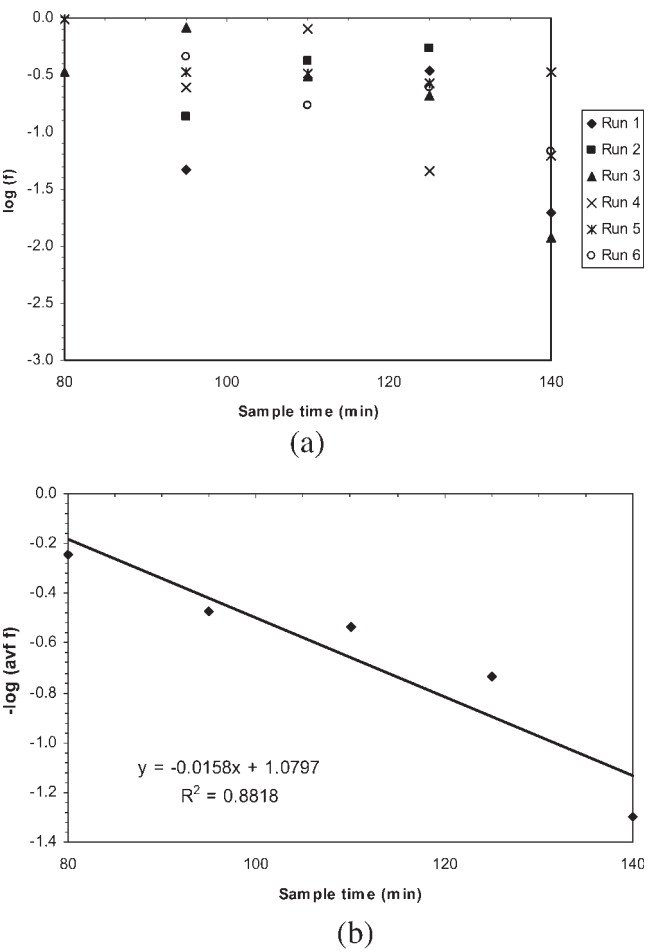

Figure 9 Initiator efficiency factor decrease of BPO in IOA microsuspensions. (A) versus time; (B) regression of average initiator efficiency versus time.

TABLE XI
IOA Emulsions with PAA (KPS Initiator)

Run #	Sample time (min)	M_n ($\times 10^{-3}$ g/mol)	M_w ($\times 10^{-3}$ g/mol)	% pseudogel	Sm. part. radius (nm) (mass %)	Lg. part. radius (nm) (mass %)
5	10				43.55 (15.86)	1803 (2.24)
	20	161.0	1981	30.7	45.93 (54.98)	1732 (16.92)
	30	132.0	2049	36.9	50.84 (68.16)	6287 (15.76)
	40	109.3	2007	36.6	55.38 (60.97)	1171 (27.10)
	60	106.0	2029	38.0	41.55 (64.46)	1673 (26.63)
	90	104.4	2026	37.11	32.85 (54.81)	8939 (38.41)
	120	109.1	2046	36.3	54.69 (78.25)	4706 (17.39)
6	20	251.2	2642	31.0	47.97 (42.15)	9194 (5.76)
	30	126.2	2020	53.4	37.57 (59.80)	2795 (20.45)
	40	147.1	2008	57.9	36.94 (59.08)	2199 (26.75)
	50	133.0	1944	57.9	30.78 (53.96)	2284 (33.27)
	60	184.0	2054	60.8	30.86 (55.46)	2880 (33.88)
	80	79.0	1611	58.5	30.88 (56.78)	5802 (34.46)
	120	120.6	1995	61.6	40.79 (73.60)	7843 (19.80)
7	30	176.3	1323	40.8	43.00 (51.49)	3993 (5.57)
	40	103.0	1906	55.7	43.76 (73.79)	6405 (7.99)
	50	130.4	1907	59.8	45.82 (71.16)	3579 (13.63)
	60	113.4	1901	59.6	30.86 (59.60)	1831 (27.85)
	80	98.6	1820	62.8	38.95 (76.29)	5605 (14.65)
	100	107.4	1804	62.5	35.47 (68.62)	9783 (23.54)
	120	84.2	1608	63.9	39.27 (70.81)	3887 (22.90)
8	20	173.7	2664	28.9	40.24 (45.18)	7284 (5.21)
	30	120.6	2247	52.0	36.34 (67.28)	6465 (19.79)
	40	212.8	2455	52.93	37.66 (71.94)	1238 (17.77)
	50	148.8	2206	53.33	38.00 (76.45)	9911 (15.01)
	60	118.1	2205	51.99	40.79 (77.51)	1854 (15.67)
	80	98.7	2246	50.28	37.08 (72.75)	1622 (21.06)
	100	125.0	2266	51.67	37.80 (72.47)	2191 (22.16)

The microsuspensions previously discussed included a hydrophobic initiator, BPO, while other formulations based on emulsion recipes used the ionic species KPS. Both recipes incorporate PAA, a water-soluble polymer used to stabilize suspensions. The presence of PAA inhibits coagulation of the supramicron particles present in the microsuspension polymerizations (with BPO). The presence of PAA in an emulsion recipe should stabilize the formation of supramicron particles deriving from nucleated monomer droplets in cases (such as IOA) where the lack of water solubility of the monomer may encourage the growth of large droplet-nucleated, rather than micellar-nucleated particles.

An comparison of the particle data in Tables XI and XII indicates that the change in initiator alters the final properties dramatically. The microsuspension polymerizations contain only small amounts of submicron particles, and the particle radii for the large particles is of the order of 20–40 μm. Variation in the mass percent small particles is thought to be insignificant. It is thought that the large particles are the result of droplet nucleation as discussed by Baker and Ketola[9]; however, it must be admitted that they could also be the result of small particle agglomeration. The oil-soluble initiator, plus the lack of water solubility of the monomer for the most part, prevents micellar nucleation. This is consistent with the work of Baker and Ketola.[9] On the other hand the emulsion with PAA employ KPS as the initiator. In this case, the large particles are more of the order of 1–2 μm radius, and more that half of the mass is in the submicron particles. This is consistent with the idea of predominant micellar nucleation caused by the water-soluble initiator. However, the low water solubility of the monomer, and the stabilizing affect of the PAA combine to make droplet nucleation significant as seen by the significant fraction of the total polymer mass in large (droplet-nucleated) particles. The large particles, however, are smaller by an order of magnitude because the growth of micellar particles has consumed the majority of the monomer originally in the monomer droplets.

Figure 10 tracks the final particle numbers for the large and small particles as a function of surfactant level for recipes containing KPS and PAA (Table XI).

TABLE XII
IOA Microsuspensions with BPO

Run #	Sample time (min)	M_n ($\times 10^{-3}$ g/mol)	M_w ($\times 10^{-3}$ g/mol)	% pseudogel	Sm. part. radius (nm) (mass %)	Lg. part. radius (nm) (mass %)
1	35	613.9	2130	1.2	315.3 (0.37)	44800 (44.66)
	45	547.2	2179	2.3	205.8 (0.36)	48040 (58.42)
	55	564.5	2170	3.0		
	65	482.8	2280	4.1	252.3 (0.33)	23770 (74.64)
	80	438.1	2001	18.7	193.5 (0.32)	27460 (82.31)
	95	457.1	2291	21.8	151.6 (0.45)	30190 (83.74)
	110	456.7	2320	23.3	164.8 (0.60)	30540 (90.11)
2	35	720.0	2400	2.12	413.5 (0.45)	30500 (41.47)
	45	868.1	2528	3.6	598.7 (0.75)	47820 (53.37)
	55	702.6	2223	3.9	436.3 (0.74)	44620 (62.60)
	65	545.3	2164	11.6	200.9 (0.46)	15530 (73.65)
	80	501.3	2197	19.1	210.7 (0.13)	23070 (82.11)
	95	505.2	2231	28.3	224.7 (0.62)	23300 (84.53)
	110	534.8	2097	30.6	274.5 (0.84)	49140 (88.02)
3	35	1043	1518	1.9	449.4 (0.60)	42280 (35.18)
	45	562.8	2343	2.9	435.7 (0.81)	38330 (47.71)
	55	569.7	2521	4.3	203.6 (0.16)	28750 (55.99)
	65	507.0	2210	4.4	436.9 (0.40)	37190 (64.40)
	80	490.9	2017	4.4	162.5 (0.45)	28240 (70.21)
	95	528.0	2071	11.4	107.5 (0.04)	21620 (77.42)
	110	428.9	2088	14.3	197.4 (0.52)	20440 (80.96)
4	35	547.4	2095	0.8	253.1 (0.08)	43100 (31.06)
	45	741.8	2196	1.6	190.1 (0.89)	34430 (45.74)
	55	583.6	2261	2.8	330.2 (0.72)	46700 (56.81)
	65	585.2	2308	3.5	145.7 (0.33)	35670 (63.83)
	80	537.9	2282	4.2	181.7 (0.17)	30480 (71.77)
	95	600.4	2301	10.3	189.6 (0.24)	32460 (75.69)
	110	524.5	2273	17.4	79.49 (0.09)	37380 (81.42)
5	35	858.8	2387	1.5	139.3 (0.44)	40810 (34.11)
	45	820.9	2305	2.3	134.0 (0.29)	29730 (46.88)
	55	735.7	2185	2.8	331.0 (1.26)	37070 (56.71)
	65	635.5	2201	4.1	169.8 (0.61)	53420 (62.43)
	80	575.0	2230	4.3	113.6 (0.80)	58900 (71.91)
	95	533.3	2170	14.1	244.8 (0.45)	65670 (76.33)
	110	498.0	2184	17.8	177.9 (0.19)	46880 (80.01)
6	35	1462	3174	5.4	232.8 (0.04)	35750 (43.43)
	45	974.6	2966	6.9	92.45 (0.22)	22280 (57.26)
	55	955.8	2818	8.2	129.5 (0.19)	25340 (66.91)
	65	723.4	2746	10.0	73.02 (0.02)	22570 (74.88)
	80	778.5	2557	16.9	100.1 (0.33)	20330 (81.46)
	95	784.6	2763	22.7	171.6 (0.19)	14410 (85.63)
	110	775.9	2782	28.9	180.9 (0.14)	18150 (87.69)

As might be expected, the small particles become the preferred locus of polymerization as the SLS is increased up to and past the CMC. These follow the same trend as the emulsion particle numbers (Fig. 4), with the transition point between the two regimes occurring at 9.8 m*M*—slightly higher than the experimentally determined CMC of 6.5 m*M*. Large particle numbers exhibit a different pattern: weak to no dependence on SLS level. Table XI reveals that these large particles are roughly an order of magnitude smaller than those in the microsuspension runs. Since the only substantive difference between the two recipes is the initiator type, this factor can be taken as being responsible for both the reduction in size and the generation of emulsion particles.

The large and small particle data for the IOA emulsions prepared with PAA are given in Table XI. It is worthwhile to investigate the extent to which the radicals partition themselves. For simplicity, it is assumed that the final mass ratio of large to small particles is representative of the amount of monomer in each size class of droplets throughout the entire

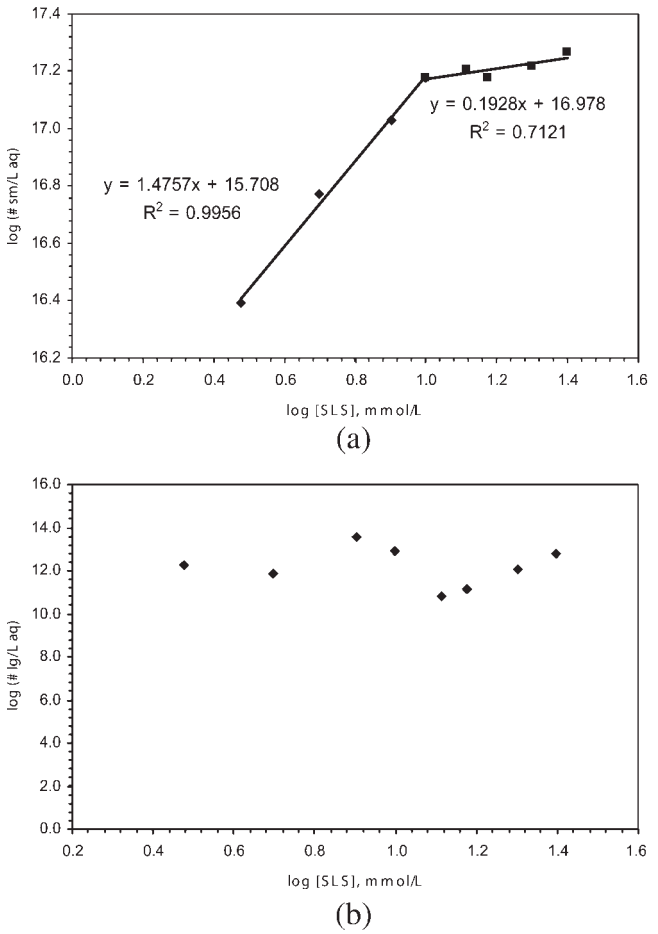

Figure 10 Final particle numbers for IOA emulsions with KPS and PAA. (A) Small particles; (B) Large particles.

reaction. This is simplistic, but allows us to estimate the number of radicals per particle for each population. Separate fractional conversions can be calculated for the large and small droplets, based on the total amount of monomer in each respective size class. Mean radicals for each size class can then be calculated from Equation (7), assuming that Smith–Ewart Interval III kinetics hold throughout. The results are shown in Figures 11 and 12. While the data is severely scattered, it is obvious that the number of radicals per particle for the small (micellar) particles is of the order of magnitude of one as would be expected, while for the large (droplet-derived) particles, it is of the order of magnitude of 100, indicating truly bulk kinetics, even though the radii of the large particles are an order of magnitude lower than for the microsuspensions.

Molecular weight distribution

By looking at the final (full conversion) molecular weight data in Tables IX–XII, some conclusions may be drawn. First, the number average molecular weights for the microsuspension polymerizations are larger by an order of magnitude than those for the emulsions and miniemulsions. However, the weight average molecular weights for all three reaction systems are approximately equal. Finally, the percentage of very high molecular weight material (''pseudogel'') is high in all three systems, but significantly lower in microsuspension than in emulsion or miniemulsion. First, since there was significant pseudogel in all cases, and since the weight average molecular weight was calculated on the total polymer *less the pseudogel*, it is not surprising that all three systems exhibited approximately the same weight average molecular weight. Second, the lower levels of pseudogel in microsuspension, coupled with the high number average molecular weights in the microsuspension would seem to indicate a lower level of branching. (Branching in these systems is most likely the result of chain transfer to polymer, followed by termination by combination.) It should be noted that the higher number average molecular weights in microsuspension compared with emulsion or miniemulsion may be an anomaly. Due to

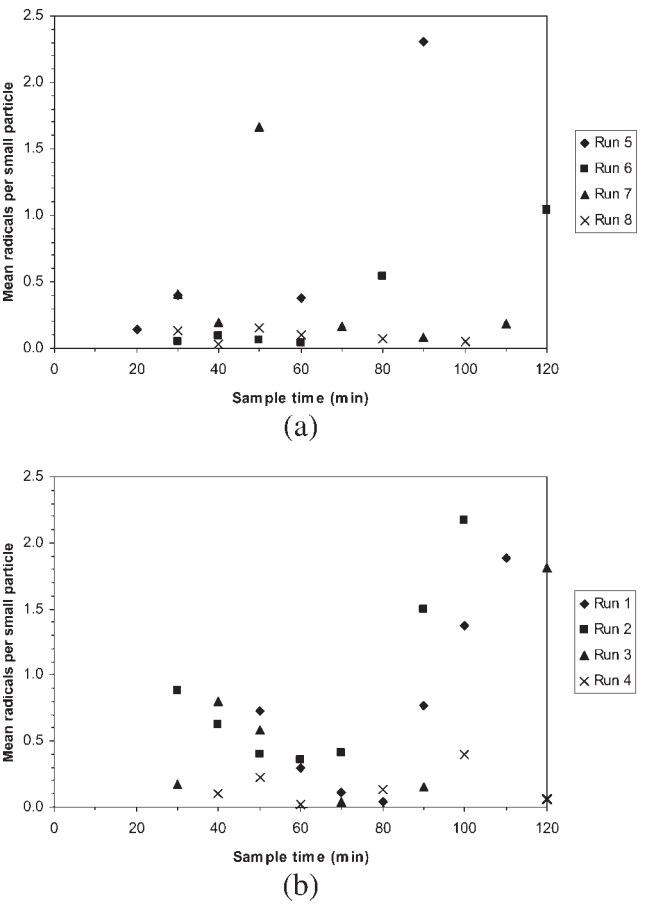

Figure 11 Mean radicals per small particle: IOA emulsions with KPS and PAA. (A) Low SLS concentrations; (B) High SLS concentrations.

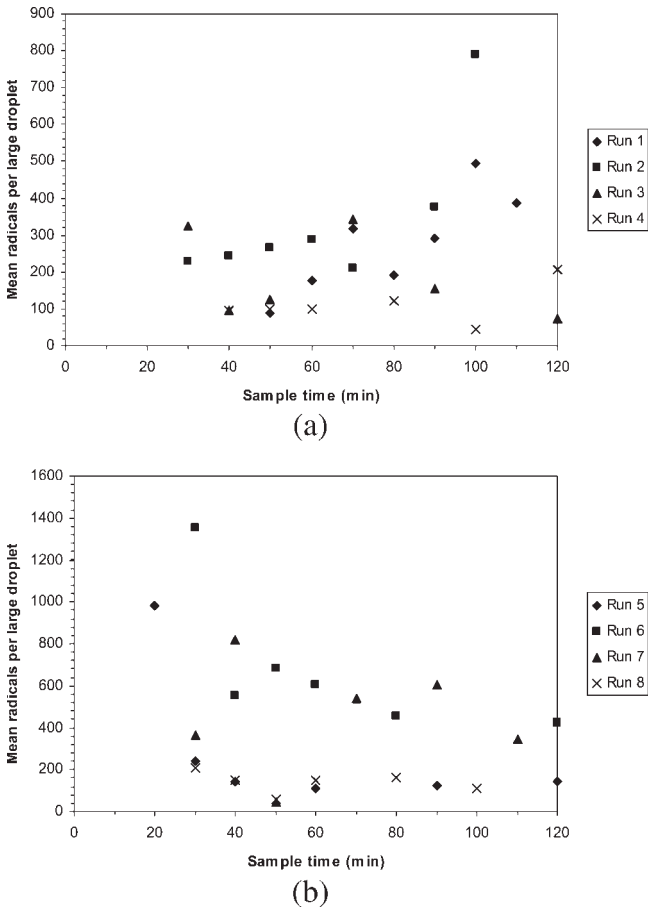

Figure 12 Mean radicals per large particle: IOA emulsions with KPS and PAA. (A) low SLS concentrations; (B) high SLS concentrations.

radical segregation, emulsion and miniemulsion systems will tend to produce higher molecular weight than bulk (suspension) systems. It may be that some of the high molecular weight polymer in the emulsion and miniemulsion samples did not go into solution, and that therefore, the molecular weights for these samples are not representative. Finally, the emulsions with KPS and PAA seem to fit between the emulsion/miniemulsion processes and the microsuspension in both number average molecular weight and percent pseudogel; this would be characteristics of a process in which micellar/small droplet nucleation (emulsion/miniemulsion) and large droplet nucleation (microsuspension) are both operative.

Summary

The results of dispersed-phase polymerization of IOA can be summarized as follows:

- The particle nucleation phenomena in emulsion and miniemulsion polymerization follow the general trends described by Vanderhoff.[12] For emulsion polymerization, as the surfactant concentration is increased, there is a transition from homogenous to micellar nucleation near the CMC, then a drop in nucleation rate at high surfactant concentration due to insufficient radical flux to support more nucleation. For miniemulsion polymerization, a slow rate of growth of (droplet) nucleation with surfactant concentration is seen, followed (at the CMC) by an increase in the rate of nucleation with added surfactant as the mode of nucleation switches to micellar.
- The conversion–time kinetics of microsuspensions can be modeled with a bulk polymerization model.
- IOA is sufficiently insoluble in the aqueous phase that emulsion polymerization may or may not be reaction limited as is always assumed for the emulsion polymerization of more water-soluble monomers.
- The presence of a stabilizer such a PAA, the use of an oil-soluble initiator such as BPO, and the insolubility of IOA in the aqueous phase all push the polymerization locus toward droplet (microsuspension) nucleation and bulk kinetics.
- The level of branching appears to be significantly less in microsuspensions of IOA than in emulsion or miniemulsion polymerization.

NOMENCLATURE

k_p	Propagation rate constant (L/mol s)
k_d	Initiator decomposition rate constant (s^{-1})
k_t	Second-order termination constant (L/mol s)
R_p	Polymerization rate (mol/L s)
k_{cM}, k_{cP}	Chain transfer constants to monomer and polymer (L/mol s)
f	Initiator efficiency
x	Fractional conversion (mass basis)
x_{conc}	Fractional conversion (based on concentration at start of Interval III)
$[M]_p$	Monomer concentration within particles (mol/L)
N_p	Particle concentration (mol/L or number/L)
ρ	First-order rate coefficient for radical capture by particles (s^{-1})
k	First-order rate coefficient for radical loss from particle (s^{-1})
N_A	Avogadro's number (mol^{-1})
V_s	Swollen particle volume (L)
t	Reaction time (s)
[mac]n	Mean active radicals per particle Particle number
N_c	Particle concentration (mol/L aq or number/L aq)

x_{conc}	Fractional conversion (based on concentration at start of Interval III)
n_M^{III}	Ratio of total moles unreacted monomer to aqueous phase volume at start of Interval III (mol/L aq)
K, a	Mark–Houwink–Sakurada parameters for polymer/solvent pair
[η]	Polymer intrinsic viscosity (dL/g)
m_M	Mass monomer in recipe (g)
V_W	Aqueous phase volume (L)
d_p	Polymer density (g/cm^3)
[mac]r	mean (unswollen) radius of particles (nm)
g	Acceleration due to gravity (m/s^2)
Δρ	Density difference, particles versus aqueous phase (g/cm^3)
μ	Aqueous phase viscosity (kg/m s)
Q_M	Maximum mass transfer rate from droplets (mol/L s)
I*, R*	Active radical
P	Monomer units that have reacted to form polymer
R	Gas constant (J/mol K)

References

1. Brandrup, J. E.; Immergut, E.; Grulke, A.; Akihiro, D.; Bloch Eds. Polymer Handbook, 4th ed.; Wiley: New York, 1999.
2. Rodriguez, F. Principles of Polymer Systems, 4th ed.; Hemisphere: New York, 1989.
3. Flory, P. J. Principles of Polymer Chemistry; Cornell University Press: Ithaca, NY, 1989.
4. Ghielmi, A.; Sorti, G.; Morbidelli, M. Chem Eng Sci 2001, 56, 937.
5. Ballard, M. J.; Gilbert, R. G.; Napper, D. H. J Polym Sci Polym Lett Ed 1981, 19, 533.
6. Lukacs, E. Probability and Mathematical Statistics; Academic Press: New York, 1972.
7. Gilbert, R. G. Emulsion Polymerization: A Mechanistic Approach; Academic Press: London, 1995.
8. Balic, R. Ph.D. Thesis, University of Sydney, Australia, 2000.
9. Baker, W. A.; Ketola, W. D. U.S. Pat. 4,166,152 (1979).
10. Perry, R. H., Ed. Perry's Chemical Engineers' Handbook, 6th ed.; McGraw-Hill: New York, 1984.
11. Vanderhoff, J. W. J Polym Sci Polym Symp 1985, 72, 168.
12. Vanderhoff, J. W. Chem Eng Sci 1993, 48, 210.
13. Reimers, J. L.; Skelland, A. H. P.; Schork, F. J. Polym React Eng 1995, 3, 235.
14. Wang, S.-T.; Poehlein, G. W. J Appl Polym Sci 1994, 51, 597.
15. Zerfa, M.; Brooks, B. W. Chem Eng Sci 1997, 52, 2423.